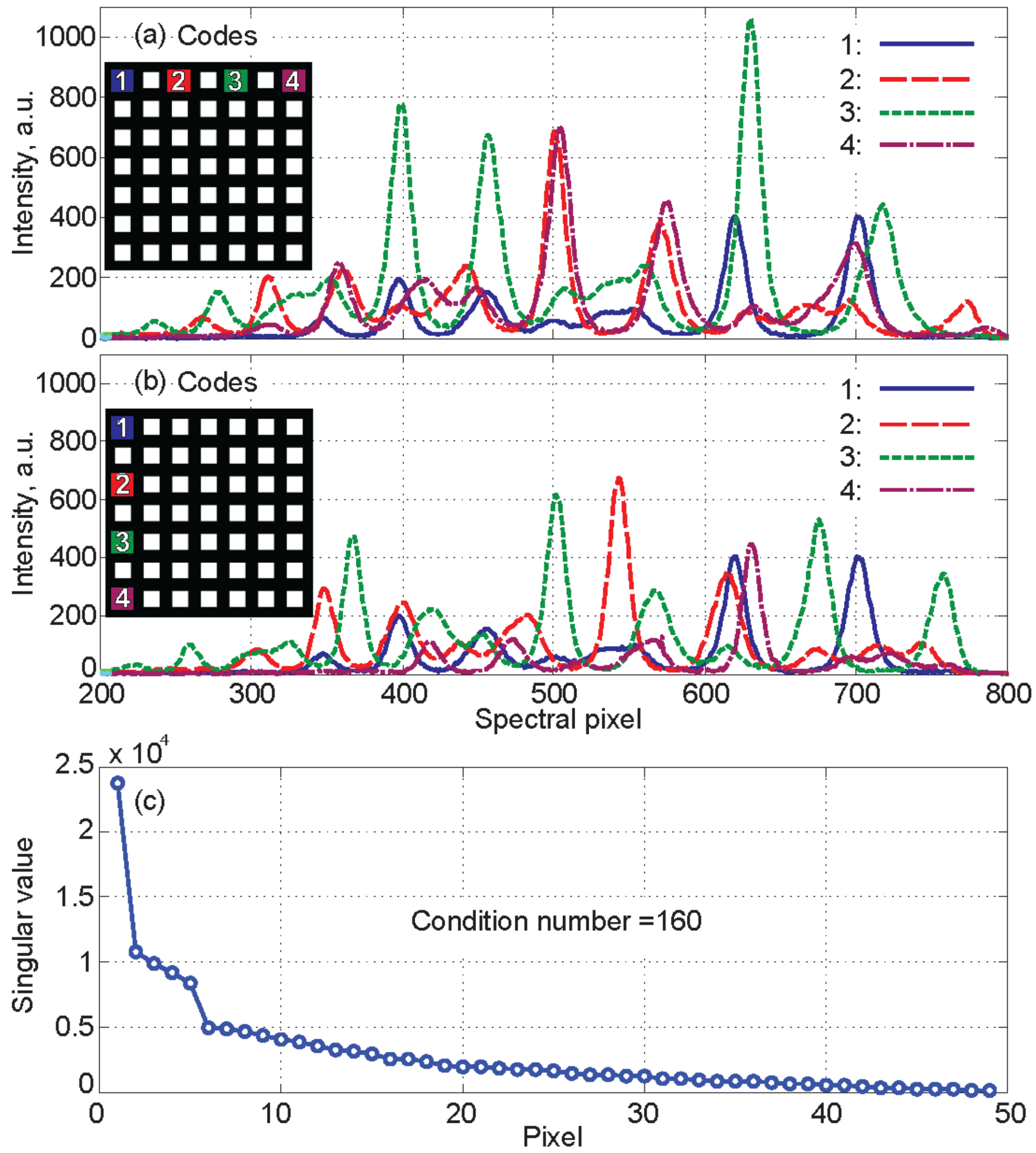

Supplementary Figure 1. Spectral codes used for object reconstruction in Fig. 3c. Intensity profiles recorded by the spectrograph, where different plot colors represent spectra obtained when the object pixels (highlighted by same color in the insets) were sequentially illuminated along (a) a row, or (b) a column. (c) Singular values obtained from the singular value decomposition of the encoding matrix M. The condition number is defined as the ratio of the largest to smallest singular value. The spectral pixel marked 500 corresponds to the wavelength 565 nm; one spectral pixel spans about 0.5 nm.

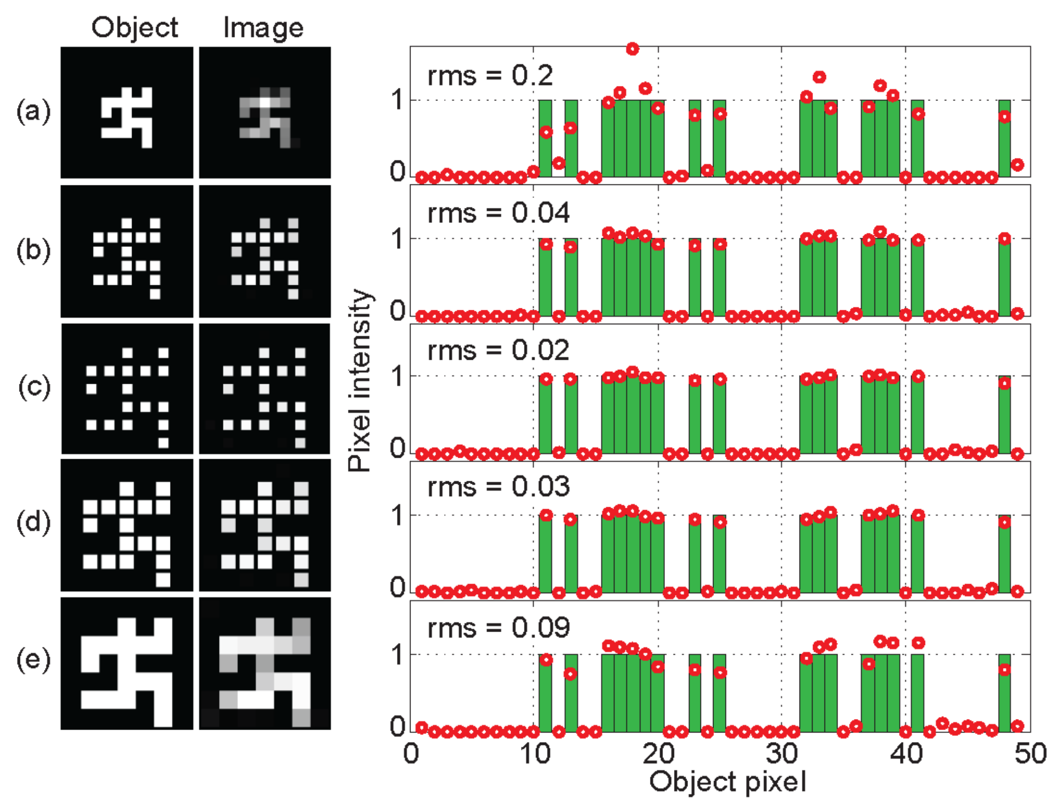

Supplementary Figure 2. Influence of pixel size and sparcity on SSE imaging. Spatially incoherent, white-light objects in the shape of a running man are sent through a SSE and launched into a fiber (see Methods). The reconstructed images and pixel values, along with the associated rms errors, are displayed for di□erent pixel layouts. In rows (a)-(c), the pixel sizes (powers) are the same, but their separation is increased, leading to better reconstruction (lower rms error). In rows (c)-(e) the pixel separations are the same, but their size is increased until the pixels are juxtaposed. The corresponding increase in pixel power is counterbalanced by a decrease in the contrast of associated spectral codes (due to increased angular diversity per pixel), leading to a net decrease in reconstruction quality (higher rms).

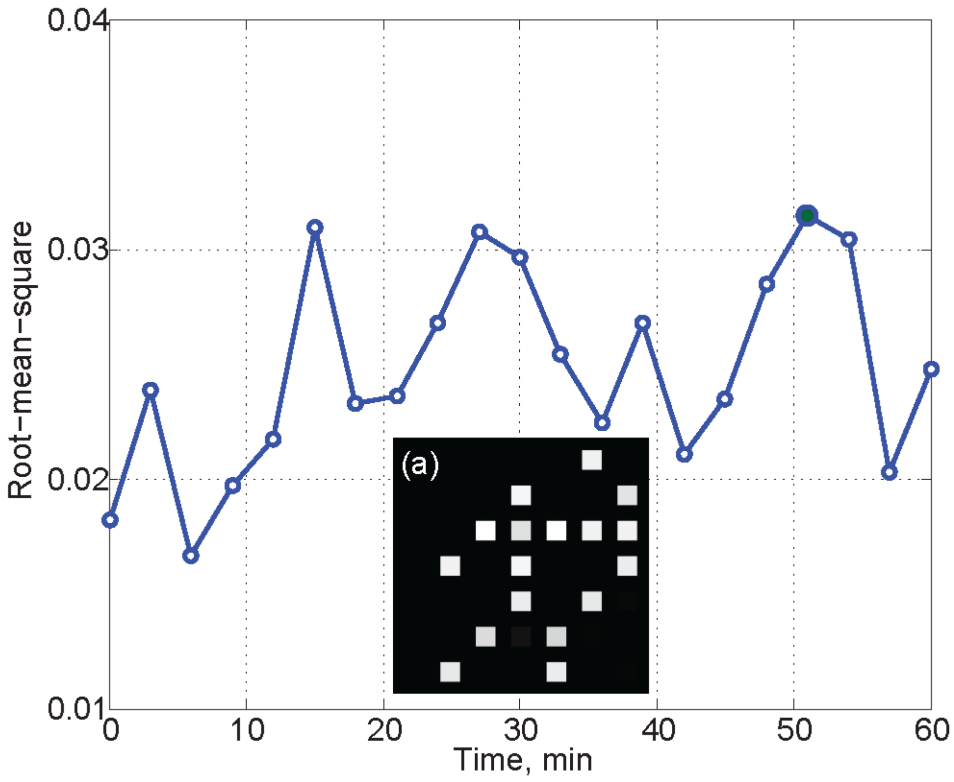

Supplementary Figure 3. Demonstration of stability of image reconstruction. Evolution of the image reconstruction quality, quantified by the root-mean-square (rms) error, as a function of time. The coding matrix measured prior to zero time was used to reconstruct an image in the shape of an archer from spectra acquired at di erent elapsed times. The inset illustrates the image reconstructed at 51 min.